Machine learning assisted Raman spectroscopy to discern the markers associated with colistin Resistance

Dimple Saikia
Department of Biosciences and Bioengineering
Indian Institute of Technology Dharwad
Dharwad, PIN: 580011, India

Cebajel Tanan
Department of Computer Science and Engineering
Indian Institute of Technology Dharwad
Dharwad, PIN: 580011, India
210010055@iitdh.ac.in

Dhananjaya G.
Department of Chemistry
Indian Institute of Technology Dharwad
Dharwad, PIN: 580011, India

Basavraj Hungund
Department of Biotechnology
KLE Technological University
Hubballi, PIN: 580031, India.

Nilkamal Mahanta
Department of Chemistry
Indian Institute of Technology Dharwad
Dharwad, PIN: 580011, India

Surya P Singh
Department of Biosciences and Bioengineering
Indian Institute of Technology Dharwad
Dharwad, PIN: 580011, India
ssingh@iitdh.ac.in

***Abstract*—Raman spectroscopy (RS) is rapidly becoming a key analytical tool for a wide range of microbiology applications. In combination with diverse machine learning methods, RS has demonstrated potentials to be translated in form of a culture-free, rapid, and objective tool for identifying antimicrobial resistance (AMR). Colistin is regarded as the final line of defence antibiotic for treating infections caused by gram-negative bacteria. In this study, we have employed a combinatorial approach of machine learning and RS to identify a novel spectral marker associated with phosphoethanolamine modification in lipid A moiety of colistin resistant gram-negative Escherichia coli. The visible spectral fingerprints of this marker have been validated by partial least square regression and discriminant analysis. The origin of the spectral feature has been confirmed by hyperspectral imaging and K-means clustering of a single bacterial cell. The chemical structure of the modified lipid A moiety has been verified by gold standard MALDI-TOF mass spectrometry. Our findings support futuristic applicability of this spectroscopic marker in objectively identifying colistin-sensitive and resistant strains.**

I. Introduction

Antimicrobial resistance (AMR) associated health crises is increasing silently and require immediate attention. It is estimated that if no proper actions are taken, it could cause 10 million deaths by 2050 and 58,000 sepsis deaths in India alone [1]. As per a report in 2020 by the Department of Biotechnology, India, and the World Health Organization, colistin is the last resort antibiotic for tackling gram-negative resistant infections. Colistin comprises of cyclic decapeptides linked to a fatty acid chain is used for treating Gram-negative infections [2]. The increased risk of antibiotic resistance towards colistin from the critical priority pathogens such as E. coli poses a potential risk to public health [3].

Lipopolysaccharides (LPS), the molecule embedded in outer-membrane of E. coli is containing of three major components: O-polysaccharide (O-antigen), core-oligosaccharide, and the lipophilic anchor part "lipid A". The vast variety of modifications such as acylation, phosphorylation, and alteration of phosphoethanolamine (PEA), in the lipid A of Gram-negative bacteria are reported [4]. V. Sándor et al. reported different structures of lipid A which can be present in E. coli. Mobile colistin resistance gene (mcr-1) codes for a transferase enzyme belonging to the family of phosphoethanolamine (PEA) transferases. Resistance to colistin primarily arises from alteration of the lipid A moiety of LPS. This modification leads to the replacement of phosphate groups of lipid A with 4'-phosphoethanolamine (PEtN) and/or cationic 4-amino-4-deoxy-L-arabinose (L-Ara4N). It leads to a decrease in the net negative charge of the LPS membrane due to blocking of phosphate and carboxyl group where colistin binds for its antibacterial action [5]–[7].

The excessive use and misuse of antibiotics have led to increased resistance against nearly all antibiotics, posing a significant threat to last-resort antibiotics such as carbapenems and colistin/polymyxins [8]–[10]. Conventional methods to identify antimicrobial resistance usually take 2-3 days due to involvement of long incubation hours and labor-intensive antibiotic susceptibility tests (AST) such as disk diffusion, e-test, or broth microdilution [11]. The long waiting time leads to more suffering for patients and increases the chances of con-

tagion. This leads healthcare professionals to use inappropriate antibiotics or sometimes prescribe broad-spectrum antibiotics, which further adds up to the problem of misuse of antibiotics. E. coli is known to be a highly evolved gram-negative bacteria that tends to become resistant against multiple classes of antibiotics including colistin [9]. The successful identification of a marker that can help in discerning between sensitive and resistant strains in a non-destructive manner has the potential to revolutionize the early screening of colistin resistance, fundamentally altering the current workflow of ASTs.

Utility of Raman spectroscopy (RS) for microbiology applications such as identification, characterization, and tracking of metabolites are widely reported due to attributes such as low-cost, label-free, fast, culture-free, and objective nature [12], [13]. Since Raman spectral data consists of large number of variables, it can be efficiently combined with different machine-learning (ML) modules to help overcome the limitations of traditional decision-making approaches and enables the forecasting of information that would otherwise be beyond the capabilities of traditional approaches.

RS coupled with ML can provides fast, effective, and objective analysis of high dimensional datasets and helps in identifying complex information and relationships among the data depending upon specific functional groups and compounds [13], [14]. This study was conducted on utilizing the exquisite molecular specificity of Raman spectroscopy in combination with different machine learning techniques to identify the alterations in the Lipid A fragment of colistin resistant E. coli as a novel spectral marker. The numerical characteristics from RS profiles were utilized to extract the features from colistin resistant microorganisms and were complemented with gold standard mass spectrometry (MS).

II. Results and discussion

A. Molecular weight characterization

The extracted Lipid A from the outer membrane of colistin-resistant and sensitive strains was analyzed by MALDI-TOF-MS to confirm the chemical modifications linked to colistin resistance (mcr-1) in comparison to the wild-type sensitive strain The typical mass-to-charge ratio (m/z) for lipid A from E. coli generally falls within the range of 1700 to 2000 Daltons [17]. Fig 1A represents protonated molecular ion [M+H]+ at 1746 Da corresponding to hexaacylated monophosphorylated lipid A from the colistin sensitive strain. The proposed structure suggest presence of GlcN disaccharide backbone having six acyl chains of 14 carbons [C4'-Phosphate, C3'-C14:O(3-O-C14:O), C2'-C14:O(3-O-C14:O), C3-C14:O(3-OH), C2-C14:O(3-OH), C1- OH] (3) [18], [19]. Colistin resistance pathogenic bacteria modify their lipid A to survive in antibiotic stress by appending phosphoethanolamine (PEA) to it. Fig 1B represents protonated molecular ion [M+H]+ at 1871 Da from the resistant strain containing modified phosphoethanolamine group at the C1 position of lipid A structure with a mass difference of 125 Da which corresponds to the mass of PEA group. On comparison of both the sensitive and resistant strain lipid A MALDI-TOF-MS data, we saw the addition of PEA in resistant strain that imparts the antibiotic resistant activity. These results further validated the successful generation of mcr-1 positive colistin resistant strains.

B. Analysis of the average Raman spectral profiles of sensitive and resistant strains

As the primary focus of this study to demonstrate the applicability of Raman spectroscopy coupled with machine learning to identify spectral markers associated with colistin resistance. In the next step Raman spectra from sensitive and resistant cells were acquired. To avoid any spectral differences caused by variations in cell number and growth phase, spectra were acquired by using an equal number of cells collected from the same growth phase [20]. The normalized mean spectra collected from E. coli strains sensitive to colistin and resistant to lower concentration of colistin (1.2 and 3.9 µg/mL) and resistant to higher concentration of colistin (6.5 and 7.8 µg/mL) is shown in Fig 2.

The shaded area indicates the standard deviation across four different experiments. The average spectra from E. coli cells resistant to ampicillin antibiotic has been used as a control to verify the molecular specificity of Raman spectroscopy. Similar to colistin the resistance mechanism for ampicillin also involves secretion of enzyme 'β-lactamase' which interferes with the binding of antibiotic to the penicillin-binding proteins (PBPs) involved in the cell wall biosynthesis. The spectral peaks at 757 cm^{-1} (phosphoethanolamine), 1130 and 1181 cm^{-1} (C-C skeletal of acyl backbone in lipids) were found to be exclusively present in E. coli cells resistant to colistin. The intensity of these bands seemed to be linearly associated with levels of colistin resistance, which could be results of higher lipids A modifications and lengthening of acyl backbone in highly resistant strains [15], [23], [24], [26]. In addition to these exclusive features typical Raman signals such as 785 cm^{-1} (nucleic acids), 1004 cm^{-1} (phenylalanine), 1094 cm^{-1} (DNA/RNA), 1245 cm^{-1} (amide III), 1337 cm^{-1} (DNA/RNA), 1450 cm^{-1} (C-H stretch), 1580 cm^{-1} (DNA/RNA) and 1659 cm^{-1} (amide I) were also observed [23]. Most of the signals were seen to be superimpositions from similar compounds for each group. Additionally, the spectral features corresponding to glycogen and various amino acids (proline, valine, hydroxyproline) in below 1000 cm^{-1} region were found to be strong in resistant cells [15], [21]. As the colistin resistance is known to be assisted by thickening of bacterial capsule via deposition of additional polysaccharide, increase in glycogen content can be expected. This is further corroborated by presence of strong features at 860, 1103 and 1740 cm^{-1} (attributed to polysaccharides and esters) [25], [26]. The visible changes in the shape of the amide I band in the resistant strains can be attributed to the structural modifications associated with induction of resistance which includes thickening of cell wall and changes in the cell shape [27]. Our previous study has demonstrated that colistin resistant E. coli cells tend to acquire a circular shape in comparison to the rod-shape of sensitive strains. Also, the induction of resistance leads to reduction in the membrane fluidity and increase in surface

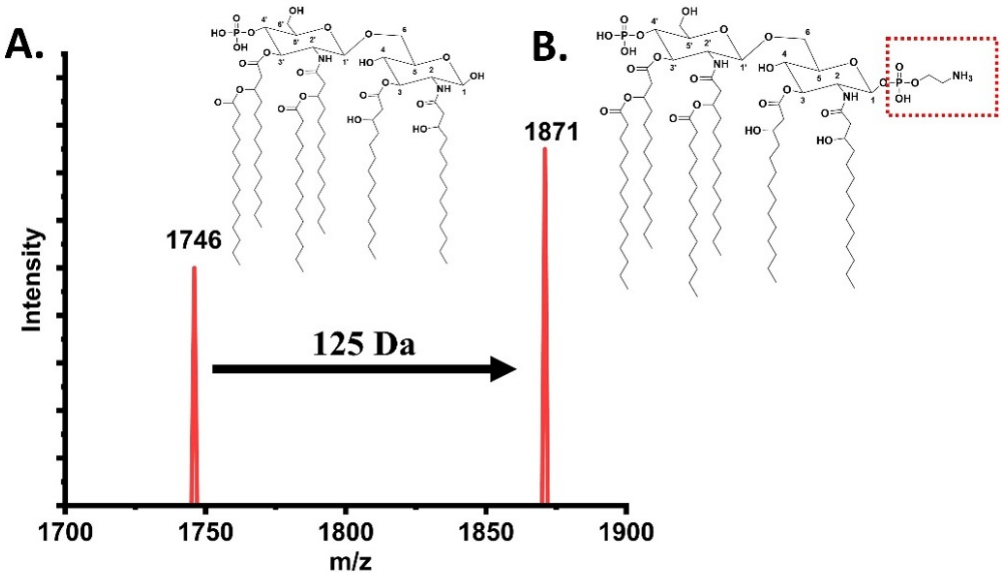

Fig. 1. Lipid-A structural difference between sensitive (A) and resistant strain (B) using MALDI-TOF-MS, PEA addition in the resistant strain indicated by the red rectangle.

roughness [20], [28], [29]. The absence of bands associated with cell wall modifications in sensitive and ampicillin control strains supports the exquisite molecular specificity of Raman spectroscopy towards identifying chemical modifications associated with colistin resistance.

C. Feature extraction and regression analysis

In the next step, to screen specific predictors that can assist in distinguishing between resistant and sensitive strains from the pool of spectral features in the 600-1800 cm^{-1} spectral range we performed PLS-DA and PLS-regression. Fig. 3A and B has the scatter plot generated from latent variables and corresponding PLS-DA coefficients.

Clear separation of the sensitive and resistance strains was observed in the scatter plot generated by the score of Factor 1 and Factor 2 of the PLS-DA model. The visible separation among the spectra appears to be contributed by both factors. The minor misclassification between sensitive and strains resistant to low colistin concentrations could be due to variability across the independent measurements. The spectral features contributing to this classification were further confirmed by the coefficient plot. It suggests that the most important variables that were positively correlated to the prediction in the PLS model were the wavenumber 757 cm^{-1} (phosphoethanolamine), 980 cm^{-1} (=CH bending from lipids), and 1131 cm^{-1} (lipids). These peaks were found to be strong in the case of colistin-resistant groups. The origin of these bands can be attributed to earlier mentioned phenomenon involving the addition of phosphoethanolamine to lipid A or disposition of extra lipopolysaccharide in the outer membrane to block the interaction between the free negatively charged phosphate groups [30]. The successful demonstration of exclusive contribution of the resistance associated spectral peaks in discrimination of sensitive and resistant strain is important with respect to the prospective adaptation this method in form of an automated resistance monitoring system.

In the next step, to explore the relationship between resistance induced spectral features and colistin concentration, a PLS regression model was developed. The primary goal of this model was to predict the antibiotic concentrations using Raman spectra as an input. The model performance was evaluated by different parameters such as MSE (mean square error), R^2 score, RMSE, and MAE (mean absolute error). The MSE measures the mean of the squared difference between predicted and actual values, which quantifies the overall accuracy of the model. The lower the MSE, the better the performance of the predicted model. The RMSE provides the average deviation between the predicted and actual values and helps to interpret the overall model accuracy; MAE represents the average of absolute differences between predicted and actual values rather than squaring them, unlike RMSE. The R^2 value explains the proportion of variance in the response values that is explained by predicted values, indicating the goodness of individual predictions. R^2 equal to 1 indicates perfect fit, and 0 indicates poor predictions [31], [32]. The value of these parameters is shown in Fig 4.

The regression model was also tested with an independent test data as shown in Fig 3C. The R^2 score of 0.89, indicating strong relationship between specific spectral variations and colistin concentrations was obtained. A closer look of the correlation plot suggests that most of the wrong predictions of this model belongs to the low resistance group specifically cells having resistance to 1.2 µg/mL of colistin. Removing this group from the regression analysis improves the overall prediction accuracy of the model significantly (R^2: 0.92; MSE: 0.81; RMSE 0.86; MAE: 0.80), Fig 4. The primary reason

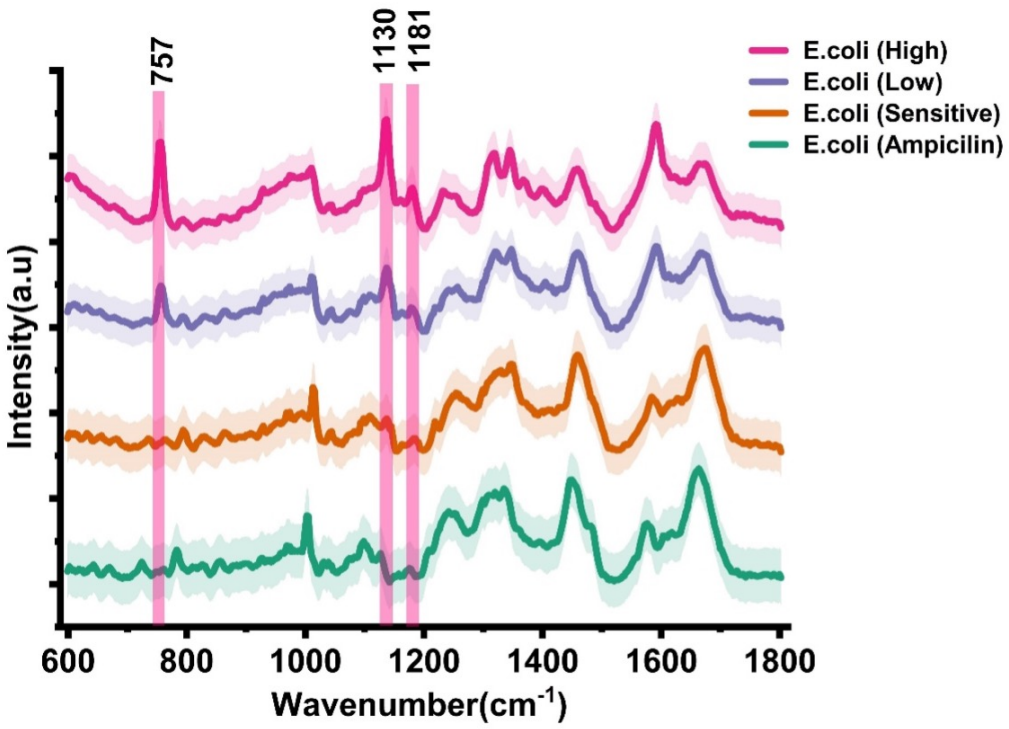

Fig. 2. Average spectra of E. coli cells ampicillin resistant, colistin-sensitive, resistant to low colistin dose and resistant to high colistin dose

for this could be attributed to the fact that cells begin to acquire specific morphological and biochemical characteristics associated with resistance at higher concentrations. This leads to origin of specific spectral signatures that can help in objectively identifying colistin resistance strains. To unravel these spectral signatures, a heat map was generated using pooled normalized spectra obtained from each group of E. coli cells sensitive to colistin, resistant to low colistin concentration, and resistant to high colistin concentration in the 600-1800 cm^{-1} range. The heat map was compared to the regression vector to analyse the presence or absence of resistance specific spectral signatures. As shown in Fig. 3D, peaks such as 757 cm^{-1}, 885 cm^{-1}, 935 cm^{-1}, 981 cm^{-1}, 1095 cm^{-1}, 1124 cm^{-1}, and 1131 cm^{-1} were prevalent in resistant strains (indicated by bright yellow). Among these the spectral features, the features around 757 cm^{-1} and 1131 cm^{-1} were prominent for colistin resistant groups, but they were found minimal for the sensitive group. These peaks were also present in the regression vector suggesting their direct involvement in accurately identifying antibiotic concentrations. The findings suggests that the correlation between intensity of these bands and antibiotic concentrations is not spurious but is due to the spectral peaks related to phosphoethanolamine modification in lipid A for colistin resistant strains.

D. Localizing the origin of spectral signals

The origin of the spectral signals was validated through hyperspectral imaging of single colistin resistant bacteria. The Fig. 5A, shows the white light optical image of the scanned area with multiple bacteria. The Raman image was constructed after pre-processing and putting an intensity filter at 2954 cm^{-1} for visualization and marking the map boundaries, Fig. 5B.

The K-means clustering analysis was performed on the Raman image and three clusters were generated. The mean spectra from each cluster were evaluated for further understanding of different origin of spectral peaks. As illustrated in Fig. 5C, clusters C1 (green) and C2 (red) correspond to the cytoplasmic content and the bacterial envelope, respectively. The cluster C3 (black) has the spectral data from the background/substrate. The average spectra from C1 and C2 were analysed to understand the major signals originating from each cluster with a focus on verifying the origin of ethanolamine modification related spectral peaks, Fig. 5D. As expected, the spectra from C1 (cytoplasm) contained mainly the vibration from DNA/RNA molecules (785 cm^{-1}), phenylalanine ring breathing mode (1004 cm^{-1}), and amide I (1664 cm^{-1}). In contrast, the spectra from C2 (bacterial envelope) had vibrations from phospholipids (1078 cm^{-1}), C-C skeletal of acyl backbone in lipids (1130 and 1181 cm^{-1}), acyl chain of lipid A (1298 cm^{-1}) and CH2 deformation of lipids (1440 cm^{-1}) [32]. The other major vibrations present in the spectra from this cluster (C2) were due to attachment of phosphoethanolamine to lipid A depicted by presence of phosphoethanolamine peak at 757 cm^{-1}. We also recorded Raman spectrum from commercially available purified phosphoethanolamine. As shown in Fig. 5E, prominent band at 757 cm^{-1} was observed. This further confirmed the origin of this band. These findings further provided conclusive evidence that exclusive spectral features

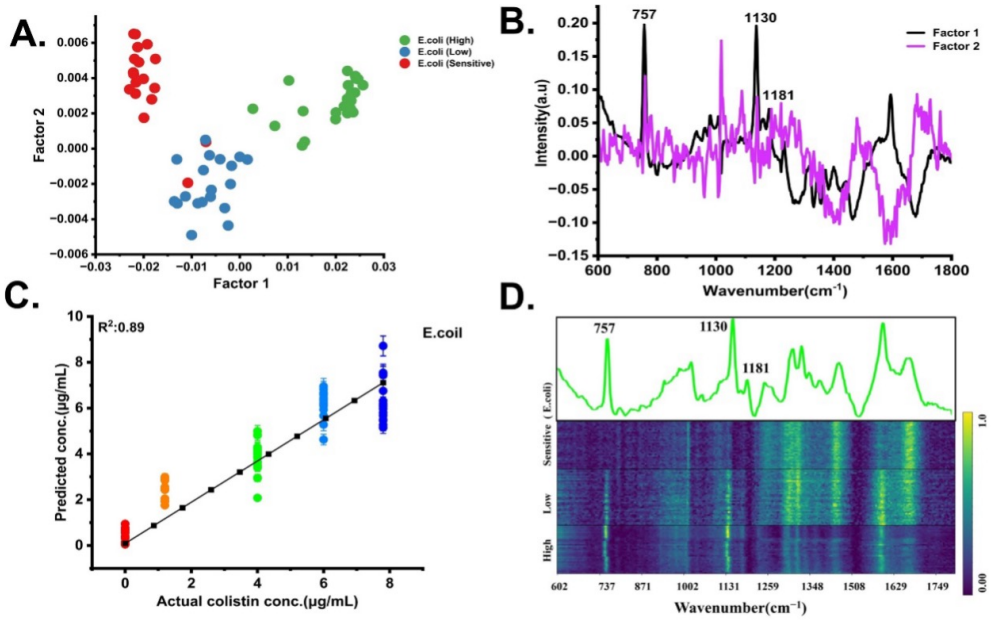

Fig. 3. (A). Partial least square discriminant analysis (PLS-DA) and corresponding coefficients (B), (C) Comparison between actual and predicted colistin concentrations through PLS regression, (D) Color coded heat map showing average spectra from all the spectra acquired from bacteria under different group. The top shows the regression vector from the prediction model. The vector plot was found to mimic the prominent spectral peaks from the colistin resistant microbes.

PLS-Regression	MSE	RMSE	MAE	R^2
All concentrations	1.35	1.16	0.97	0.89
Without 1.2 µg/mL	0.81	0.86	0.80	0.92

Fig. 4. Performance evaluation of the PLS-regression model via independent test data set.

associated with lipid A modifications localized in the outer membrane region of the colistin resistant bacteria could be successfully identified using Raman imaging.

Optical spectroscopic approaches specifically Raman based methods have demonstrated significant potential to be used as adjunct tools for different kinds of microbiology applications. As the colistin resistance is associated with specific chemical changes in the outer membrane of the bacterium, we aimed to identify specific markers that are associated with these modifications. In summary, the results indicate that Raman spectroscopy can effectively detect spectral changes associated with phosphoethanolamine appendage in lipid A for colistin resistance strains. Hyperspectral imaging revealed that the spectral features specific to colistin resistance originated from the outer membrane of the bacterial cells. At higher antibiotic concentrations the prediction accuracy of these models was found to be extremely good (R^2= 0.92). The overall findings are suggestive of prospective adaptation of this combinatorial approach of Raman spectroscopy and machine learning to monitor the specific markers associated with colistin resistance.

E. Experimental Microbial strains

The laboratory grown colistin resistant strains of E. coli were created by mobile colistin resistance gene (mcr-1) gene transformation. Single colonies of colistin-resistant and sensitive strains and inoculated in LB-broth culture medium with appropriate antibiotic concentrations. A library of colistin resistant E. coli ranging between 1.2 µg/mL to 7.8 µg/mL was created [15].

F. Lipopolysaccharide (LPS) extraction and MALDI-TOF-MS analysis of Lipid A

LPS was extracted from E. coli colistin sensitive (wild type) and resistant (mcr-1 positive) using LPS extraction kit (MAK339) purchased from Sigma Aldrich. E. coli colistin sensitive and resistant were initially plated on the agar medium and incubated for 18 hrs at 37°C. A single colony was picked from sensitive and resistant strains and inoculated in 100 ml of LB-broth overnight with and without antibiotics, respectively. At the OD600 of 0.6, the bacterial cells were pelleted by centrifugation at 5000 rpm for 10 minutes and the supernatant was discarded. Cell pellets were washed with cold PBS (pH 7.2) and then the weight of the cells was measured. Briefly the

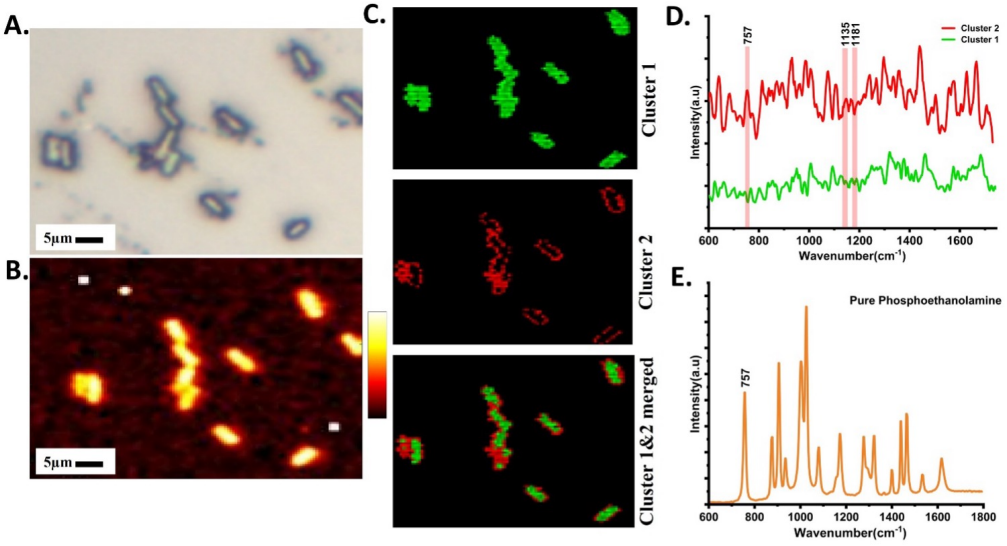

Fig. 5. Localization of resistant specific spectral signatures: (A) The white light image of the bacterial cells, B) Visualization and understanding of the overall bacterial map using signal at 2954 cm^{-1} (C) K-means clustering analysis from Raman signal obtained from bacteria (D) Mean spectra from each of clusters. Peaks corresponding to ethanolamine modification and long lipid chain are marked. (E) Raman spectra from pure phosphoethanolamine

LPS extraction process was consisting of treatment with lysis buffer (100 µl lysis buffer for 10 mg of cells pellet) followed by sonication for complete lysis of the cells at 20 sec(3X) in continuous pulse at 10 watts keeping the tubes in ice followed by 10 mins incubation on ice. Then samples were centrifuged at 5000 rpm for 10 mins in 4°C. The lysate was collected in a new tube and 5 µl of proteinase K (1 µl proteinase K for 20 mg of cell mass) was added to each tube and incubated at 60°C for 1hr. This was followed by centrifugation (5000 rpm, 10 mins at 4°C) then transfer of the supernatant (total LPS) to a new 1.5 mL micro-centrifuge tube. This extracted total LPS was subjected to hydrolysis with 10 µl of 1% acetic acid followed by heating the samples at 100°C for 1 hour to obtain lipid A. Finally, lipid A extraction was done by using chloroform, methanol, and water at 3:2:0.25 ratio. The samples were centrifuged, and the chloroform layer (bottom) was collected which contains the lipid A [16]. Lipid A was concentrated using a vacuum concentrator until completely dry. Finally, the lipid A samples were dissolved in chloroform and mixed with 2,5-Dihydroxybenzoic acid (DHB) matrix and were analysed using a RapifleX Matrix assisted laser desorption ionization (MALDI)-time of flight (TOF)-mass spectrometry (MS) instrument (Bruker Daltonics, Germany). The spectra were obtained in the reflectron positive ion mode. The analyses were performed at the mass spectrometry facility, Division of Biological Sciences, IISc, Bangalore, India.

G. Raman spectra acquisition and preprocessing

Spectra were collected from both colistin-resistant and sensitive strains of E. coli. Among the resistant strains, two had low resistance levels (1.2-3.9 µg/mL), while the other two were highly resistant to colistin (6.5-7.8 µg/mL). Additionally, spectra from the sensitive strain were also collected. To prepare the samples for Raman spectra acquisition, the resistant strains were inoculated in presence of appropriate colistin concentration, and the sensitive strains were inoculated without antibiotic and incubated at 37ºC until O.D600 reached to 0.6-0.8. Cells were pelleted via centrifugation at 10,000 rpm for 3 mins, followed by washing using chilled PBS to remove traces of culture media. The experiments were repeated four times maintaining the same conditions. The washed microbial pellets were transferred to a sterilized CaF2 window, and spectra were obtained using WITec alpha300 Raman microscope. The system is equipped with a 532 nm laser, grating 600 groove/mm, cooled charged coupled device, and a 100 X objective with 0.8 numerical aperture. The spectra were acquired at a power of 20 mW with an exposure time of 5 sec and averaged over 3 accumulations. The Raman spectra were imported to MATLAB software for data analysis in the fingerprint region 600-1800 cm^{-1}. The background contributions from substrate and culture media were removed. Data from each group was pre-processed via removing of cosmic spikes, polynomial fitting for baseline correction, and unit normalization.

H. Data analysis

After preprocessing spectra were divided in to three groups: sensitive, low, and high resistance to colistin. To visualize the spectral differences, the mean spectra was calculated by averaging the variables on the Y axis keeping the same X-axis (wavenumber). PLS-DA was utilized to reduce the dimensions of the data by extracting the latent variables to obtain the maximum variations in the spectra. The first step of PLS-DA modelling was the construction of PLS components for dimensionality reduction. As a result of this algorithm, the original data was rearranged to a low-dimensional subspace

as scores (PLS-DA score) with highest covariance with class labels. The regression coefficient evaluates the performance of the PLS-DA model. The positive coefficient indicates strong influence of the corresponding variables on the discrimination between the classes. The relationship between the Raman spectra collected from different groups: sensitive, low (1.2 and 3.9 µg/mL), and high (6.5 and 7.8 µg/mL) was established using a partial least squares regression (PLS-R) model. The model performance was validated based via regression coefficients, mean squared error (MSE), root-mean-square error (RMSE), and R^2 score for the independent test data. These parameters provide insights into the accuracy, precision, and goodness of fit of regression models. The data analysis was performed using Python (scikit-learn package). Each group had a series of recorded spectra collected on different days, considering possible variations while keeping the same instrumental and Raman configuration parameters. The entire analysis pipeline employed in this study is shown Fig 6.

I. Single cell hyperspectral imaging for localization of spectral signal

Microbial cells were spread on a CaF2 window to obtain single cell and imaging was performed using previously mentioned WITec alpha 300 microscope equipped with Zeiss epiplan 100 X objective (NA 0.8, WD 1.3 mm). The average laser excitation power was 20 mW with exposure time of 2 seconds. Total scan area was 25×25 µm (width × height) consisting of 100 points per line and 100 lines per image, with step size of 0.25 µm. Routine preprocessing steps such as cosmic removal and Savitzky-Golay smoothening was performed on the Raman images. The image outline was confirmed using filter on 2954 cm^{-1}. This was followed by K-means cluster analysis (CA) to partition the data into nearest centroids-based distance matrix. The Euclidean distance clustering algorithm was used to create the final clusters. Each cluster was represented by a single mean spectrum. The mean spectra were filtered and baselined corrected.

III. Conclusions

The findings of the study further support the prospective utility of machine learning based Raman spectroscopy methods for identifying markers of colistin resistance. Prospective adaption of the proposed approach can provide an alternate/adjunct tool for identifying antibiotic resistance in short and clinically implementable time.

IV. Author contributions

D.S., S.P.S conceived and designed the project. D.S, T.C.B performed experiments and data analysis. D.G, N.M conducted MALDI analysis. B.H supplied strain. All the authors wrote and corrected the manuscript. S.P.S acquired the funding and directed the research.

V. Conflicts of interest

There are no conflicts to declare.

VI. Data availability

The data that supports the findings of this study is available from the corresponding author upon reasonable request.

VII. Acknowledgements

This work was carried out under research grant project no (37/1739/23/EMR-II) supported by Council of Scientific and Industrial Research (CSIR), Government of India and project no. IIRP-2023-1734 from Indian Council of Medical Research (ICMR), Government of India. Dhananjaya G. acknowledges Prime Minister Research Fellowship (PMRF- 1502705), Government of India.

References

[1] Laxminarayan R, Duse A, Wattal C, Zaidi AK, Wertheim HF, Sumpradit N, Vlieghe E, Hara GL, Gould IM, Goossens H, Greko C, So AD, Bigdeli M, Tomson G, Woodhouse W, Ombaka E, Peralta AQ, Qamar FN, Mir F, Kariuki S, Bhutta ZA, Coates A, Bergstrom R, Wright GD, Brown ED, Cars O, "Antibiotic resistance-the need for global solutions," Lancet Infect Dis. 2013 Dec;13(12):1057-98.

[2] Falagas ME, Kasiakou SK, "Colistin: the revival of polymyxins for the management of multidrug-resistant gram-negative bacterial infections," Clin Infect Dis. 2005 May 1;40(9):1333-41.

[3] Sharma, Sarin, S, "Indian Priority Pathogen List. 2019,"Available online: https://cdn.who.int/media/docs/default-source/searo/india/antimicrobial accessed on 10 September 2022)

[4] Klein G, Müller-Loennies S, Lindner B, Kobylak N, Brade H, Raina S, "Molecular and structural basis of inner core lipopolysaccharide alterations in Escherichia coli: incorporation of glucuronic acid and phosphoethanolamine in the heptose region," J Biol Chem. 2013 Mar 22;288(12):8111-8127

[5] Yi-Yun Liu, Yang Wang, Timothy R Walsh, Ling-Xian Yi, Rong Zhang, James Spencer, Yohei Doi, Guobao Tian, Baolei Dong, Xianhui Huang, Lin-Feng Yu, Danxia Gu, Hongwei Ren, Xiaojie Chen, Luchao Lv, Dandan He, Hongwei Zhou, Zisen Liang, Jian-Hua Liu, Jianzhong Shen, "Emergence of plasmid-mediated colistin resistance mechanism MCR-1 in animals and human beings in China: A microbiological and molecular biological study," Lancet Infect Dis, vol. 16, no. 2, pp. 161–168, 2016.

[6] K. Novović and B. Jovčić, "Colistin Resistance in Acinetobacter baumannii: Molecular Mechanisms and Epidemiology.," Antibiotics (Basel), vol. 12, no. 3, Mar. 2023, doi: 10.3390/antibiotics12030516.

[7] A. B. Janssen and W. van Schaik, "Harder, better, faster, stronger: Colistin resistance mechanisms in Escherichia coli," PLoS Genet, vol. 17, no. 1, pp. 1–4, 2021.

[8] Li, B., Yin, F., Zhao, X., Guo, Y., Wang, W., Wang, P., Zhu, H., Yin, Y., & Wang, X., "Colistin Resistance Gene mcr-1 Mediates Cell Permeability and Resistance to Hydrophobic Antibiotics," Front Microbiol, vol. 10, Jan. 2020.

[9] De Oliveira DMP, Forde BM, Kidd TJ, Harris PNA, Schembri MA, Beatson SA, Paterson DL, Walker MJ, "Antimicrobial Resistance in ESKAPE Pathogens," Clin Microbiol Rev, vol. 33, no. 3, pp. 10.1128/cmr.00181-19, May 2020.

[10] A. N. Schuetz, "Antimicrobial Resistance and Susceptibility Testing of Anaerobic Bacteria," Clinical Infectious Diseases, vol. 59, no. 5, pp. 698–705, Sep. 2014.

[11] Gajic I, Kabic J, Kekic D, Jovicevic M, Milenkovic M, Mitic Culafic D, Trudic A, Ranin L, Opavski N,"Antimicrobial Susceptibility Testing: A Comprehensive Review of Currently Used Methods," Antibiotics, vol. 11, no. 4, 2022.

[12] L. Ashton, K. Lau, C. L. Winder, and R. Goodacre, "Raman spectroscopy: lighting up the future of microbial identification," Future Microbiol, vol. 6, no. 9, pp. 991–997, Sep. 2011.

[13] Wang Liang , Liu Wei , Tang Jia-Wei , Wang Jun-Jiao , Liu Qing-Hua , Wen Peng-Bo , Wang Meng-Meng , Pan Ya-Cheng , Gu Bing , Zhang Xiao, "Applications of Raman Spectroscopy in Bacterial Infections: Principles, Advantages, and Shortcomings," Frontiers in Microbiology, vol. 12. Frontiers Media S.A., Jul. 19, 2021.

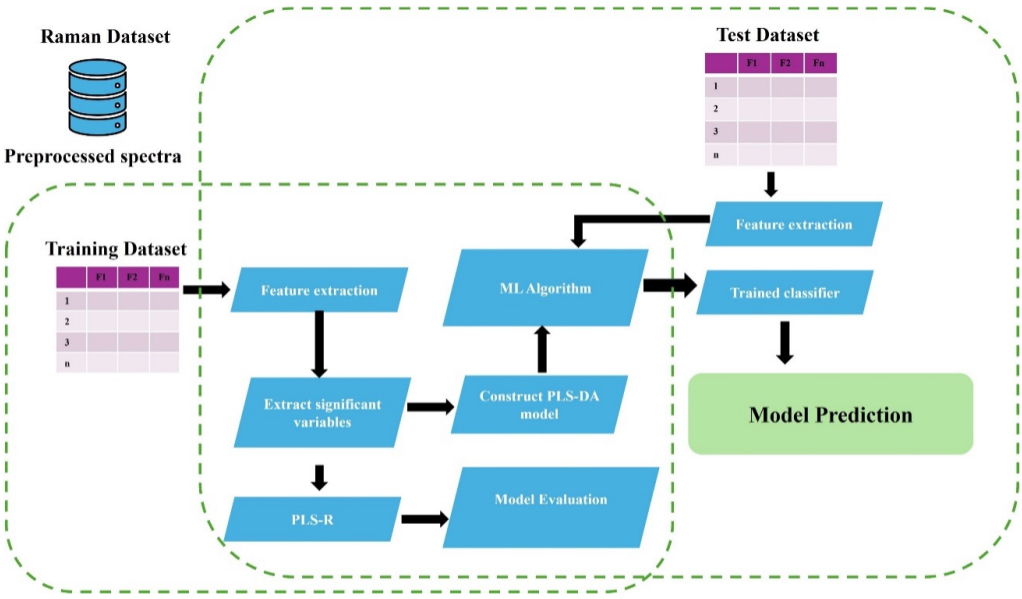

Fig. 6. Illustration of the generalized pipeline employed in this study.

[14] Popa SL, Pop C, Dita MO, Brata VD, Bolchis R, Czako Z, Saadani MM, Ismaiel A, Dumitrascu DI, Grad S, David L, Cismaru G, Padureanu AM, "Deep Learning and Antibiotic Resistance," Antibiotics (Basel). 2022 Nov 21;11(11):1674.

[15] D. Saikia, P. Jadhav, A. R. Hole, C. M. Krishna, and S. P. Singh, "Unraveling the Secrets of Colistin Resistance with Label-Free Raman Spectroscopy," Biosensors (Basel), vol. 12, no. 9, Sep. 2022.

[16] Bligh Eg, Dyer Wj, "A rapid method of total lipid extraction and purification" J Biochem Physiol 1959 Aug; 37(8):911-7.

[17] Lee CS, Kim YG, Joo HS, Kim BG, "Structural analysis of lipid A from Escherichia coli O157:H7:K- using thin-layer chromatography and ion-trap mass spectrometry," J Mass Spectrom. 2004 May;39(5):514-25.

[18] M. Kurogochi and S.-I. Nishimura, "Structural Characterization of N-Glycopeptides by Matrix-Dependent Selective Fragmentation of MALDI-TOF/TOF Tandem Mass Spectrometry," Anal Chem, vol. 76, no. 20, pp. 6097–6101, Oct. 2004.

[19] V. Sándor, A. Kilár, F. Kilár, B. Kocsis, and Á. Dörnyei, "Characterization of complex, heterogeneous lipid A samples using HPLC–MS/MS technique II. Structural elucidation of non-phosphorylated lipid A by negative-ion mode tandem mass spectrometry," Journal of Mass Spectrometry, vol. 51, no. 8, pp. 615–628, Aug. 2016.

[20] Saikia D, Jadhav P, Hole AR, Krishna CM, Singh SP. Growth Kinetics Monitoring of Gram-Negative Pathogenic Microbes Using Raman Spectroscopy. Appl Spectrosc. 2022 Oct;76(10):1263-1271.

[21] C. Krafft, L. Neudert, T. Simat, and R. Salzer, "Near infrared Raman spectra of human brain lipids," Spectrochim Acta A Mol Biomol Spectrosc, vol. 61, no. 7, pp. 1529–1535, May 2005.

[22] Lin, Z.; Zhao, X.; Huang, J.; Liu, W.; Zheng, Y.; Yang, X.; Zhang, Y.; de la Chapelle, M.L.; Fu, W, "Rapid screening of colistin-resistant Escherichia coli, Acinetobacter baumannii and Pseudomonas aeruginosa by the use of Raman spectroscopy and hierarchical cluster analysis," Analyst 2019, 144.

[23] A. C. S. Talari, Z. Movasaghi, S. Rehman, and I. Rehman, "Raman Spectroscopy of Biological Tissues," Appl Spectrosc Rev, vol. 50, no. 1, pp. 46–111, Jan. 2015.

[24] Gogry, F, Siddiqui, M.T.; Sultan, Husain, F.M., Al-Kheraif, A.A.; Ali, A. Haq, Q.M.R, "Colistin Interaction and Surface Changes Associated with mcr-1 Conferred Plasmid Mediated Resistance in E.coli and A.veronii Strains," Pharmaceutics 2022, 14, 295.

[25] Monika Dudek, Grzegorz Zajac, Ewelina Szafraniec, Ewelina Wiercigroch, Szymon Tott, Kamilla Malek, Agnieszka Kaczor, Malgorzata Baranska, "Raman Optical Activity and Raman spectroscopy of carbohydrates in solution," Spectrochim Acta A Mol Biomol Spectrosc, vol. 206, pp. 597–612, Jan. 2019. 26. P. D. A. Rohs and T. G. Bernhardt, "Annual Review of Microbiology Growth and Division of the Peptidoglycan Matrix," Annual Review of Microbiology, (2021), 315-336, vol. 75.

[26] P. D. A. Rohs and T. G. Bernhardt, "Annual Review of Microbiology Growth and Division of the Peptidoglycan Matrix," Annual Review of Microbiology, (2021), 315-336, vol. 75.

[27] M. Hartmann, M. Berditsch, J. Hawecker, M. F. Ardakani, D. Gerthsen, and A. S. Ulrich, "Damage of the bacterial cell envelope by antimicrobial peptides gramicidin S and PGLa as revealed by transmission and scanning electron microscopy," Antimicrob Agents Chemother, vol. 54, no. 8, pp. 3132–3142, Aug. 2010.

[28] R. L. Soon, R. L. Nation, P. G. Hartley, I. Larson, and J. Li, "Atomic force microscopy investigation of the morphology and topography of colistin-heteroresistant Acinetobacter baumannii strains as a function of growth phase and in response to colistin treatment," Antimicrob Agents Chemother, vol. 53, no. 12, pp. 4979–4986, Dec. 2009.

[29] John CM, Liu M, Phillips NJ, Yang Z, Funk CR, Zimmerman LI, Griffiss JM, Stein DC, Jarvis GA, "Lack of lipid A pyrophosphorylation and functional lptA reduces inflammation by Neisseria commensals," Infect Immun. 2012 Nov;80(11):4014-26.

[30] Beveridge TJ, "Structures of gram-negative cell walls and their derived membrane vesicles," J Bacteriol. 1999;181(16):4725-4733.

[31] D. Chicco, M. J. Warrens, and G. Jurman, "The coefficient of determination R-squared is more informative than SMAPE, MAE, MAPE, MSE and RMSE in regression analysis evaluation," PeerJ Comput Sci, vol. 7, pp. 1–24, 2021.

[32] H. Abdi, "Partial Least Squares (PLS) Regression." Available: http://www.utdallas.edu/